

# Magnetic field induced luminescence spectra in a quantum cascade laser

V.M. Apalkov and T. Chakraborty

*Max-Planck-Institut für Physik Komplexer Systeme, Dresden, Germany*

We report on our study of the luminescence spectra of a quantum cascade laser in the presence of an external magnetic field tilted from the direction perpendicular to the electron plane. The effect of the tilted field is to allow novel optical transitions because of the coupling of intersubband-cyclotron energies. We find that by tuning the applied field, one can get optical transitions at different energies that are as sharp as the zero-field transitions.

The unipolar quantum cascade laser (QCL) [1–3] is the product of ingenious quantum engineering that exploits the properties of electrons confined in semiconductor nanostructures. As yet, this is the only high power semiconductor laser that operates at and above room temperature in the mid-infrared range [4–9]. Intense interest on this system derives from its technological importance in trace-gas analysis, in particular, for environmental control, remote chemical sensing, pollution monitoring, non-invasive medical diagnostics, etc. [7]. Here we study the novel effects of a tilted magnetic field on a QCL where the coupled intersubband-cyclotron transitions are allowed [10,11]. We find that as the subbands quantize into discrete Landau levels, new luminescence peaks appear that correspond to those transitions. The peaks exhibit a prominent red shift but can be made as sharp and large as the zero-field case by tuning the applied field.

The system we have studied here is sketched schematically in Fig. 1, where a GaInAs quantum well of 7.4 nm width is sandwiched between two AlInAs tunneling barriers. When a suitable bias is applied, electrons tunneling through the upstream barrier generate photons and escape quickly to the next well through the downstream barrier. Superlattice structures on both sides of the active region act as electron injector or Bragg mirrors and control the rate of electron escape [1–3]. The operating wavelength of the lasers is determined by the quantum confinement rather than the bandgap of the materials.

An externally applied magnetic field tilted from the direction perpendicular to the electron plane is a well-studied problem experimentally as well as theoretically, in the context of quantum Hall effects [10]. For a magnetic field tilted from the  $z$  direction the perpendicular and parallel motions of electrons are coupled and as a result, transitions between different Landau levels of the ground and upper subbands become possible. Interestingly, the perpendicular component of the tilted field provides magnetic quantization, somewhat analogous to the situation proposed for a quantum-dot cascade laser [12,13] where the quantization of the planar motion is due to replacement of the quantum wells by quantum dots [14]. The Hamiltonian of the system in a tilted field is

$$\mathcal{H} = \mathcal{H}_\perp + \mathcal{H}_\parallel + \mathcal{H}'$$

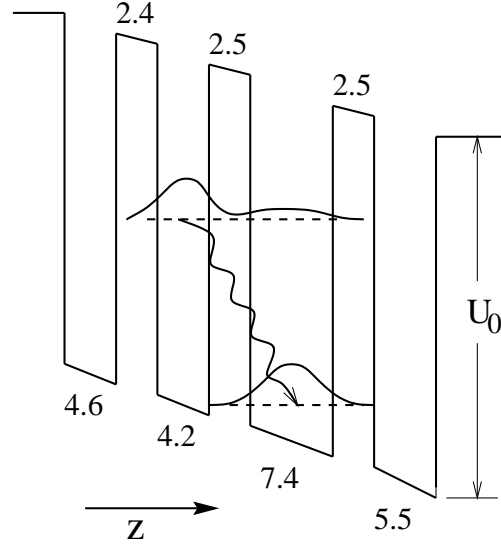


FIG. 1. Energy band diagram (schematic) of the active region of a quantum cascade laser structure under an average applied electric field of 55 kV/cm. Only one period of the device is shown here. The relevant wave functions (moduli squared) as well as the transition corresponding to the laser action are also shown schematically. The numbers (in nm) are the well (Ga<sub>0.47</sub>In<sub>0.53</sub>As) and barrier (Al<sub>0.48</sub>In<sub>0.52</sub>As) widths. Material parameters considered in this work are: electron effective mass  $m_e^*$  (Ga<sub>0.47</sub>In<sub>0.53</sub>As)=0.043  $m_0$ ,  $m_e^*$  (Al<sub>0.48</sub>In<sub>0.52</sub>As)=0.078  $m_0$ , the conduction band discontinuity,  $U_0 = 520$  meV, the nonparabolicity coefficient,  $\gamma_w = 1.3 \times 10^{-18}$  m<sup>2</sup> for the well and  $\gamma_b = 0.39 \times 10^{-18}$  m<sup>2</sup> for the barrier, and the sheet carrier density induced by doping,  $n_s = 2.3 \times 10^{11}$  cm<sup>-2</sup>. The energy difference between the two levels where the optical transition takes place, is 132 meV. All computations were performed at  $T = 50$  K.

where

$$\begin{aligned}\mathcal{H}_\perp &= \frac{1}{2m^*} p_z^2 + V_{\text{eff}}(z) + \frac{\hbar^2}{2m^*} \frac{z^2}{\ell_\perp^4} \\ \mathcal{H}_\parallel &= \frac{1}{2m^*} \left[ p_x^2 + \frac{\hbar^2}{\ell_\perp^4} (x + X)^2 \right] \\ \mathcal{H}' &= \frac{\hbar}{m^*} \frac{z p_x}{\ell_\parallel^2}\end{aligned}$$

with  $X \equiv \frac{p_y}{\hbar} \ell_\perp^2$  the center coordinate of the cyclotron motion and  $\ell_\parallel^2 = c\hbar/eH_y$ ,  $\ell_\perp^2 = c\hbar/eH_z$  are the magnetic lengths. Here we have chosen the Landau gauge vector potential,  $\mathbf{A} = (H_y z, H_z x, 0)$ . The magnetic field is therefore in the  $y - z$  plane and  $H_y = H \sin \theta$ ,  $H_z = H \cos \theta$ ,  $\theta$  is the tilt angle and  $H$  is the total magnetic field [10].

The effective potential is made up of the (i) confinement potential, (ii) Hartree potential, and the (iii) exchange-correlation potential [15]. The wave functions of the Hamiltonian  $\mathcal{H}_\perp$ , which depend only on  $z$ -coordinate are obtained from

$$\mathcal{H}_\perp \psi_n = E_n \psi_n(z).$$

Solutions of this equation determine the energy levels and wave functions of the subbands. The total Hamiltonian is diagonalized by choosing the basis wave functions

$$\begin{aligned}\Psi_{n,N,X} &= L^{-\frac{1}{2}} \exp\left(-i\frac{X}{y}\ell_\perp^2 - i\frac{z_{nm}}{\ell_\parallel^2}(x - X)\right) \\ &\quad \times \xi_N(x - X)\psi_n(z) \\ \xi_N(x) &= i^N (2^N N! \pi^{\frac{1}{2}} \ell_\perp)^{-1/2} H_N\left(\frac{x}{\ell_\perp}\right) \exp\left(-\frac{x^2}{2\ell_\perp^2}\right) \\ z_{nm} &= \int dz \psi_n(z) z \psi_m(z)\end{aligned}$$

where  $H_N(x)$  is the Hermite polynomial. The Hamiltonian matrix elements  $\langle n'N'X'|\mathcal{H}|nNX\rangle$  are then calculated in this basis. The matrix is diagonal in  $X$ . To calculate the wave functions we use three subbands and 20 Landau levels on each subband.

Once we diagonalize the Hamiltonian the chemical potential is then obtained from the equation

$$N_s = \frac{2}{2\pi\ell_\perp^2} \sum_N \frac{1}{\exp(\beta(E_{2,N} - \mu)) + 1}$$

where  $E_{2,N}$  is the energy of  $N$ -th Landau level in the second subband (only the second subband is occupied). The optical spectra are calculated as follows [11]: Optical transitions occur between Landau levels of the second and first subbands. We introduce the variables that are proportional to matrix elements of optical transitions

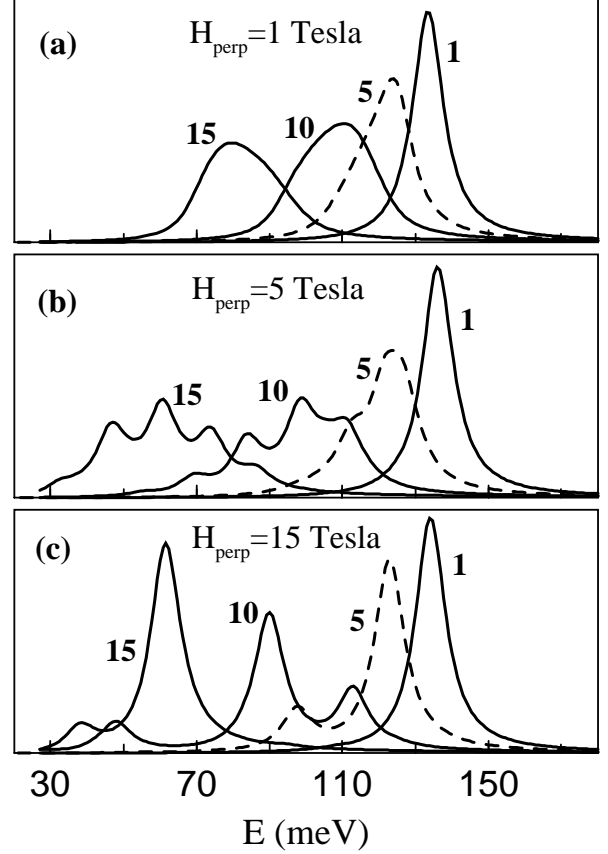


FIG. 2. Luminescence spectra at various values of the parallel component of the magnetic field (numbers by the curves in tesla) for a fixed value of the perpendicular component of the field.

$$\begin{aligned}u_{(N,N_1)} &= \frac{1}{eF} \left(\frac{2m^*}{\hbar^2}\right)^{-\frac{1}{2}} \frac{(1, N|\mathcal{H}^*|2, N_1)}{(E_{2,N_1} - E_{1,N})^2 - (\hbar\omega)^2} \\ &\quad \times \{f(E_{2,N_1})\}^{\frac{1}{2}}\end{aligned}$$

where  $\mathcal{H}^*$  is the change of Hamiltonian due to an external electric field  $F$  in the  $z$  direction, and  $f(\varepsilon)$  is the Fermi distribution function. Note that we consider the first subband as empty. The emission spectrum is related to  $u_{(N,N_1)}$  through

$$\mathcal{I}(\omega) \propto \omega \frac{1}{2\pi\ell_\perp^2} \sum_{N,N_1} z_{1,2} \{f(E_{2,N_1})\}^{\frac{1}{2}} \Im(u_{(N,N_1)})$$

where  $\omega$  is the frequency of the emitted photon.

Intensity of the optical emission is determined by the dipole matrix elements between initial (before emission) and final (after emission) states of the multi-electron system. In dipole transitions the transition intensity is proportional to the overlap between  $(x, y)$ -dependent parts of the wave functions of the initial and final states [14]. For a vanishing perpendicular magnetic field this results

in conservation of the two-dimensional momentum in the optical transition. For non-zero perpendicular magnetic fields the states of the two-dimensional electrons are classified by two numbers: the Landau level index and by a number that distinguishes the degenerate states of an electron within a Landau level, for example, by  $x$  component of the momentum. The energy of the single electron system depends only on the number of the Landau level, and the wave functions are harmonic oscillator functions whose center is determined by the  $x$  component of the momentum. If the magnetic field is directed perpendicular to the two-dimensional layer then optical transitions are allowed only between the states with the same two-dimensional quantum numbers. In this case we will have a single line which corresponds to the optical transitions between states with the same Landau level index.

Introduction of a non-zero parallel magnetic field in  $y$  direction results in modification of the wave function in a Landau level: the position of oscillator wave functions is now determined by  $y$  component of the momentum and also by average position of the electron in  $z$  direction,  $\langle z \rangle$  that depends on the number of subbands. Figure 1 illustrate this dependence. Electrons in the first subband and in the second subband are localized in the quantum wells 7.4 nm and 4.2 nm, respectively. This opens up the possibility for optical transitions between different Landau levels and at the same time it suppresses the optical transitions between the states with the same Landau level indices.

Evolution of the emission spectra as a function of the tilted magnetic field and tilt angle are illustrated in Figs. 2 and 3. In Fig. 2, the optical spectra are shown for three values of the perpendicular component of the field and for different values of parallel component of field for a fixed  $H_{\text{perp}}$ . Clearly, for small  $H_{\text{perp}}$  (Fig. 2a), the emission spectra do not feel the Landau quantization and we have a single peak which broadens with increasing  $H_{\text{par}}$ . For higher fields such as  $H_{\text{perp}} = 5$  tesla (Fig.2b), we find new features in the emission spectra. For a small parallel field,  $H_{\text{par}} = 1$  tesla, main transitions are between the states with the same Landau index, hence a single peak that corresponds to transitions from the zeroth Landau level of second subband to that of the first subband. An increase of the parallel field makes transitions to higher Landau levels more intense. Appearance of a shoulder at  $H_{\text{par}} = 5$  tesla corresponds to transitions to the first Landau level of the first subband. Similarly, peaks at  $H_{\text{par}} = 10$  tesla and 15 tesla correspond to transitions from zeroth Landau level of the second subband to the higher Landau level of the first subband. The energy separations between the peaks are equal to the separations between Landau levels of the first subband. In Fig. 2c, transitions to non-zero Landau level become more intense and we observe an interplay between the transitions to zero and to the first Landau levels with increasing parallel field. For a small  $H_{\text{par}}$  ( $H_{\text{par}} = 1$  tesla), there is only

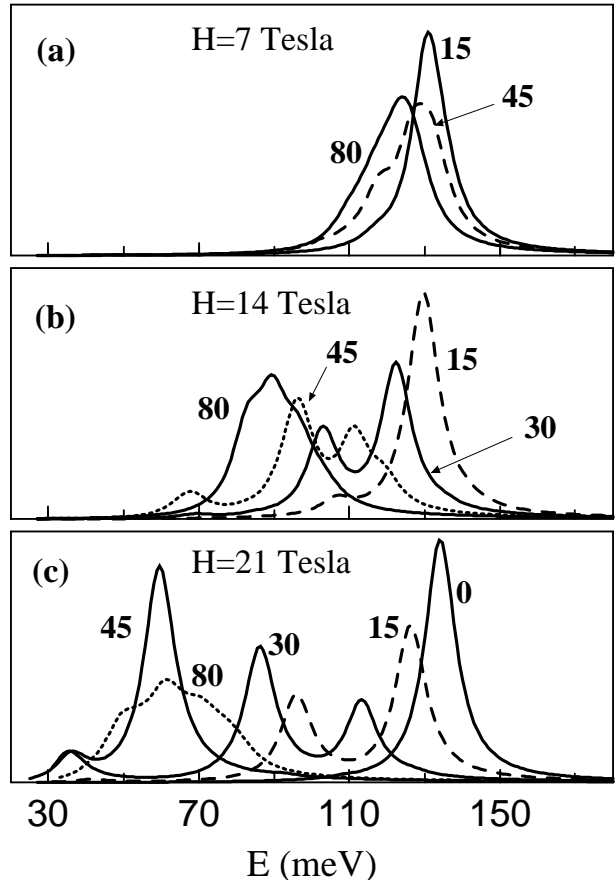


FIG. 3. Luminescence spectra at various values of the tilt angle (numbers by the curves) for a fixed value of the total magnetic field.

a strong transition to zeroth Landau level. For  $H_{\text{par}} = 5$  tesla, we observe the appearance of a small peak that corresponds to transitions to the first Landau level, and for  $H_{\text{par}} = 10$  tesla and 15 tesla, transitions to the first Landau level become strongest and we observe the formation of a new narrow peak that corresponds to a transition to the first Landau level.

In a recent experiment by Blaser et al. [16], QCL based on photon-assisted tunneling transition was subjected to a parallel field of upto 14 tesla. The luminescence spectra showed a broadening of the peak but almost no shift (a very tiny blue shift was observed) with an increasing parallel field. Broadening of the luminescence peak with increasing parallel field is also visible in Fig. 2(a) where the perpendicular field is rather small, but the experimentally observed broadening is much more rapid. In addition, there is a strong red shift in Fig. 2(a) that is not visible in the observed spectra. In the present scheme, a red shift seems to be quite natural in the single-electron picture [17,18]. The change of the wave function due to

a parallel field ( $H_{\text{par}} < 10$  tesla) is small for the first and the second subbands. Magnetic field changes the energy spectrum because of a shift of the parabolic energy dispersion by a value that is proportional to the field. This results in a broadening and red shift of the emission spectrum without the many-body effects. The many-body effects changes the results only slightly and results in a blue shift ( $\sim 4$  meV) of the emission spectra that is independent of the applied magnetic field. The observed total intensity of emission line gets smaller with higher parallel fields. At 10 tesla, it is smaller than its value at zero field ( $I_0$ ) by 45% ( $0.55 I_0$ ) [19]. In contrast, our calculated values indicate a reduction by 16% ( $0.84 I_0$ ).

In our present scheme, the small blue shift (or almost absence of any shift) observed in [16] in a strong parallel field cannot be explained by many-body corrections, because these corrections in samples of [16] are small and have a weak magnetic field dependence. The weak magnetic field dependence of many-body effects was also demonstrated in [20] for much wider quantum wells (30-46 nm) where one expects even larger magnetic field dependence than for narrow wells. One possible explanation of the observed results of [16] might be due to the presence of disorder in the system which tends to localize the two-dimensional electrons [21] and thereby break the conservation of momentum in the optical emission. Magnetic field tends to delocalize the states which can result in a decrease of emission intensity and widening of the emission lines. Our present results would, of course, be valid for disorder-free high-mobility systems.

In Fig. 3, the emission spectra are shown for three values of the total magnetic field  $H$  and for different values of the tilt angle at a fixed  $H$ . For a small field (Fig. 3a) we have a red shift of the emission spectra with increasing parallel field (i.e., increasing tilt angle). For  $\theta = 45^\circ$  there is a weak structure resulting from the Landau quantization. At higher fields (Fig. 3b,c), one observes the evolution of the emission spectra from a broad peak at a large angle,  $\theta = 80^\circ$ , (large parallel field and a small perpendicular field) to a single narrow peak for small angle. In the latter case, the parallel component of the magnetic field is small and all optical transitions are transitions between the Landau levels with the same index. For an intermediate tilt angle, there are two peaks that correspond to transitions from the zeroth Landau level of the second subband to zeroth and the first Landau levels of the first subband. The intensity of transition to the first Landau level increases with increasing angle which means an increase of the parallel field. It has its maximum at  $\theta = 45^\circ$  and for total magnetic field of  $H = 21$  tesla one observes the formation of a strong narrow peak at  $\theta = 45^\circ$  associated with a suppression of the original peak corresponding to the transition to zeroth Landau level of the first subband. This is the same peak as shown in Fig. 2 for  $H_{\text{perp}} = H_{\text{par}} = 15$  tesla. From these results, we conclude that by suitably tuning the externally applied

tilted field, lasing due to coupled intersubband-cyclotron transitions that is as strong as the zero-field case (but at different energies) can be achieved. Although for the present system the magnetic fields where the novel transitions take place are rather high, by suitably engineering the device parameters these transitions can be made to occur at lower fields.

We would like to express our gratitude to P. Fulde for his kind support and for valuable discussions. We also thank S. Blaser for helpful discussions and for his unpublished results.

- 
- [1] J. Faist, et al., *Science*, **264**, 553 (1994).
  - [2] J. Faist, et al., *Appl. Phys. Lett.*, **66**, 538 (1995).
  - [3] J. Faist, et al., *Nature*, **387**, 777 (1997).
  - [4] J. Faist, et al., *Appl. Phys. Lett.*, **72**, 680 (1998).
  - [5] C. Gmachl, et al., *Electron Lett.*, **34**, 1103 (1998).
  - [6] J. Faist, et al., *Appl. Phys. Lett.*, **68** 3680 (1996).
  - [7] J. Faist, et al., *IEEE Photon. Technol. Lett.*, **10**, 1100 (1998).
  - [8] C. Sirtori, *Appl. Phys. Lett.*, **73**, 3486 (1998).
  - [9] P.T. Keightley, et al., *Physica E*, **7**, 8 (2000).
  - [10] T. Chakraborty, and P. Pietiläinen, *The Quantum Hall Effects* (Springer, New York, 1995, 2nd edition).
  - [11] T. Ando, *Phys. Rev. B*, **19**, 2106 (1979).
  - [12] C.F. Hsu, et al., *SPIE*, **3001**, 271-281 (1997).
  - [13] N.S. Wingreen and C.A. Stafford, *IEEE J. Quantum Electron.*, **33**, 1170 (1997).
  - [14] T. Chakraborty, *Quantum Dots* (North-Holland, Amsterdam, 1999).
  - [15] D.M. Ceperley, and B.J. Alder, *Phys. Rev. Lett.*, **45**, 566 (1980).
  - [16] S. Blaser, *Physica E*, **7**, 33 (2000).
  - [17] T. Ando, *J. Phys. Soc. Jpn.*, **44**, 475 (1978).
  - [18] W. Beinvoogl, A. Kamgar, and J.F. Koch, *Phys. Rev. B*, **14**, 4274 (1976).
  - [19] S. Blaser, unpublished results (2000)
  - [20] R.H.J. De Meester, et. al., *Physica E*, **7**, 93 (2000).
  - [21] C. Metzner, et. al., *Phys. Rev. B*, **58**, 7188-7196 (1998).